15TH IEA HEAT PUMP CONFERENCE
MAY 26–29, 2026 | HOFBURG
VIENNA 2026
DECARBONISATION THROUGH INNOVATION

Effects of Variable Borehole Thermal Resistance and Heat Pump Behavior on Sizing and Energy Consumption of a Swedish Residential Ground-Source Heat Pump System

Timothy N. West[a], Jeffrey D. Spitler[a*], Signhild Gehlin[b]

[a]Oklahoma State University, Stillwater, OK, 74078 USA
[b]Swedish GeoEnergy Center, Lund, SE-233 55, Sweden

Abstract

Ground-source heat pump systems are commonly used to provide space heating and domestic hot water in Swedish residential buildings. Design and energy analysis of these systems are commonly done assuming constant borehole thermal resistance and fixed heat pump COP, ignoring the impact of backup electric resistance heating. Since most Swedish boreholes are groundwater filled, the borehole thermal resistance tends to increase when the groundwater in the borehole approaches the maximum density point of water, about 4°C. Under cold conditions, the heat carrier fluid inside the U-tube may also drop into laminar flow, increasing the thermal resistance of the boreholes. Modern water-source heat pumps with variable speed compressors and circulating pumps may have COP and, hence, heat extraction rates that vary significantly over the year. Backup electric resistance heating may also affect sizing of the borehole heat exchanger. It is therefore expected that borehole sizing, heat pump energy consumption, and economics may be affected by the level of detail used in modeling the system. This paper describes improvement in borehole heat exchanger and heat pump modeling and examines the effects on sizing, prediction of energy use, and economics, for a house in Sweden.

Selection and/or peer-review under the responsibility of the organizers of the 15th IEA Heat Pump Conference 2026.

Keywords: Ground-source heat pump, geothermal heat pump, ground heat exchanger design

1. Introduction

Ground source heat pump (GSHP) systems are commonly used for space heating and domestic hot water (DHW) heating in Swedish residential buildings. Every fourth Swedish single-family house has a GSHP installed [1]. The typical Swedish GSHP system is an electrically driven monovalent fluid-to-water heat pump connected to a vertical groundwater filled borehole drilled in crystalline rock, with a single U-tube borehole heat exchanger (BHE) using an ethanol-water mix as heat carrier fluid suspended in the groundwater. Back-up heating for peak load is often provided by an electric resistance heater inserted in the integrated water tank.

The performance of a BHE depends on the thermal properties of the ground and the materials used inside the borehole, as well as the BHE geometry, which may be represented as a borehole thermal resistance. Design tools and energy analysis software for calculation of GSHP systems typically assume that the borehole thermal resistance of the BHE is fixed. While this assumption may be valid for grouted boreholes, such as are used in the USA and continental Europe, this does not apply for groundwater filled boreholes, which is common practice in Sweden and other Scandinavian countries.

In groundwater filled boreholes, the borehole thermal resistance tends to decrease with higher borehole temperatures and increase when the groundwater in the borehole approaches the maximum density point of water, about 4°C [2]. Kjellsson and Hellström [3] investigated the effect of convection in boreholes with water outside the pipes, in a laboratory study with a polyethylene single U-tube inserted in a temperature controlled-water filled outer tube. They observed substantial reduction of borehole thermal resistance (50%) at fluid

* Corresponding author. *E-mail address:* spitler@okstate.edu

temperatures above 35°C and heat injection rates larger than 50 W/m. Gustafsson et al. [4] analyzed the effect of natural convection in groundwater filled boreholes in hard rock using a 3D steady-state CFD model. Several field studies using thermal response tests e.g. [5, 6], confirm the effect of natural convection on the borehole thermal resistance in groundwater filled boreholes. Spitler, et al. [7] present experimental measurements from a single well-instrumented borehole under a range of heat transfer rates and annulus temperatures, where Nusselt numbers for natural convection in the annulus are correlated against modified Rayleigh number. Spitler, et al. [8] used the convection correlations from that study to develop a calculation tool for computing local and effective thermal resistances of single U-tube borehole heat exchangers in vertical boreholes for either grouted or groundwater-filled boreholes. Todorov, et al. [9] compare the convection correlations with several methods for evaluating and modelling the effective thermal resistance in groundwater-filled boreholes, based on distributed temperature sensing (DTS) measurements of six of the boreholes in a bore field with a total of 74 boreholes. The boreholes were 300 m deep and fitted with single U-tubes and mean fluid temperatures were measured over 39 months. They observed that the effective thermal resistance may vary significantly during operation.

Borehole thermal resistance is also influenced by the flow conditions inside the BHE tubes. Under cold conditions, the heat carrier fluid inside the U-tube may drop into laminar flow due to the temperature dependent increase of the fluid viscosity. Laminar flow conditions dramatically increase the thermal resistance of the boreholes. Gehlin and Spitler [10] discussed trade-offs between GSHP system design and supplementary electric resistance heating by simulating 10 years operation of a Swedish single-family house with DHW and space heating provided by a GSHP system. The same GSHP system simulation tool was used by Gehlin and Spitler [11] in a study of the effects of flow velocity on the heat pump system performance in two backfilled BHE with a single U-tube in South Dakota in USA. The results suggested that, from an overall system performance perspective, it is more important to keep a low ground loop pressure loss than to maintain flow high enough to ensure turbulent flow at all times of the year. Javed and Spitler [12] present an experimental study of pressure loss versus flow for a single U-tube and three other borehole heat exchanger types in a groundwater filled 200 m deep vertical borehole in hard rock. Procedures for calculating the pressure loss for these borehole heat exchanger types were tested and the effects of using fiber optic cable assemblies inserted into the pipe were investigated, including correlations for the excess pressure loss due to the optic fibers.

Operating hours when the groundwater temperature in groundwater filled BHE is around 4°C and thus has limited natural convection movement in the BHE water typically occur in the GSHP peak load season. It is also in peak load hours that the heat carrier fluid temperature is as lowest, resulting in the highest risk for laminar flow conditions inside the U-tube. Because these GSHP systems often use backup electric resistance heating, and this heating may occur at peak electric grid conditions, it is expected that the prediction of energy use and emissions is sensitive to variations in the borehole thermal resistance. Spitler, et al. [13] simulated a range of GSHP system designs with different BHE designs and heat pump capacities serving a Swedish single-family house with back-up electric resistance heater, to estimate hourly electricity consumptions and CO2-emissions.

BHE in Sweden are commonly designed assuming a fixed borehole thermal resistance and a fixed heat pump coefficient of performance (COP) that dictates how much heat extraction is required for any building heating load. The fixed borehole thermal resistance is often estimated based on assuming an effective water thermal conductivity of 1.25 W/(m·K) and a spacing between each leg of the U-tube and the wall that is equal to the spacing between the two legs of the U-tube. The borehole thermal resistance would then be calculated with the multipole method [14]. Heat pump performance, and, hence, the ratio of heat extraction to heating also varies throughout the year. This is particularly the case for modern heat pumps with variable speed compressors and variable-speed pumping.

The focus of this paper is investigation of the effect of variable borehole thermal resistance on the design, energy consumption, and estimation of operating cost on a typical Swedish residential GSHP system. The results indicate that the simpler simulations lead to shorter borehole lengths, but fully detailed simulations predict energy consumptions about 14% lower than those predicted by the simpler simulations .

2. Methodology

In order to investigate the sensitivity of the simulation results, design, and energy consumption, a system serving a prototypical house located in Nynäshamn, 60 km south of Stockholm on the Swedish Baltic coast, is simulated.

2.1. Heating Loads

The prototypical house is based on an actual house built in the 1930s, with some energy efficiency retrofits performed. The house has a basement and two above ground floors, with a total area of 140 m^2. The EnergyPlus simulation was calibrated to actual utility bills for 2023 & 2024. Domestic hot water loads are on a typical daily schedule supplied with BeOpt [15], with a total hot water draw of 262 L/day and heating load of about 9 kWh/day. With the calibrated building description, building heating loads are determined for a typical meteorological year [16], as shown in Figure 1.

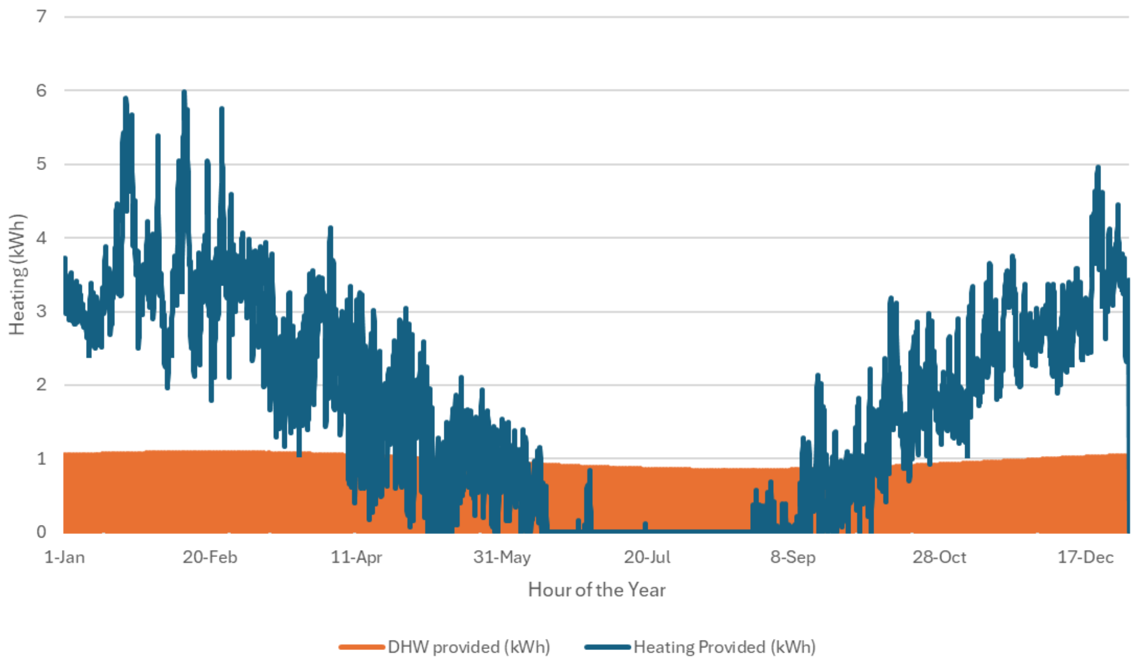

Figure 1. Hourly heating loads for the Nynäshamn house.

2.2. Heat Pump Model

The heat pump model is based on a commercially available variable-speed Calibra 7 [17] heat pump manufactured by Thermia with a nominal 7 kW heating capacity. The manufacturer provides heating capacity, input power, and COP in two tables, as a function of 5 compressor speeds, 3 brine temperatures and two load-side supply temperatures. The heat pump model may be divided into four parts – (1) a model of heating capacity, input power and COP for any combination of compressor speed, brine temperature, and load-side supply temperature, and (2) a control curve that sets the required load-side supply temperature based on outdoor air temperature, and (3) supervisory control that adjusts the compressor speed, directs heating to either the building or domestic hot water, and, if necessary, activates the backup electric resistance heating, and (4) control of the circulating pumps that varies the pump speed to provide constant temperature difference across the borehole.

The first part uses generalized least squares to determine the heating capacity (Q_{cap}) utilizing Equation 1. The capacity was fit with five coefficients ($C_{h,0}$ through $C_{h,4}$) and depends on the GHE entering fluid temperature (T_{brine}), the exiting temperature of the load-side fluid (T_{supply}), and the compressor speed (ω).

$$Q_{cap} = C_{h,0} + C_{h,1}T_{brine} + C_{h,2}T_{supply} + C_{h,3}\omega + C_{h,4}\omega^2 \tag{1}$$

A similar equation is fit to represent COP; power is determined by taking the ratio of heating provided to the COP. The effectiveness of these fits is discussed in section 3.1.

A control curve is commonly used in Swedish residential systems. In practice, it is adjusted to ensure satisfactory comfort in the individual house. We used a typical control curve given by Björk, et al. [18]. For domestic hot water, a supply temperature of 55°C is used.

For each hour, with the desired load-side supply temperature set by the control curve, the supervisory control determines heating capacity for building heating and domestic hot water heating, then calculates the hourly run-time fraction required for building heating and for domestic hot water heating at the maximum compressor speed. If the sum of the run-time fractions exceeds one, electric resistance heating is used to supplement the vapor compression cycle. If the heat pump has more than enough capacity at the highest compressor speed but not enough capacity at lowest compressor speed, then the supervisory control determines required compressor speed to run the entire hour at an intermediate speed. If the heat pump has more than enough capacity at the lowest compressor speed, it is cycled on and off to meet the loads at the lowest compressor speed.

The heat pump's brine flow rate is controlled (by adjusting the circulating pump speed) to give a temperature difference of 3°C, and the model mimics this.

2.3. Borehole Heat Exchanger Model

The borehole heat exchanger is typical for a single-family residential system in Sweden – a single, groundwater-filled borehole surrounded by granite. For this paper, the grouted and groundwater filled boreholes both consist of a single 32mm SDR 17 U-tube circulating a 24% ethanol solution The model is a custom, hourly time-step model that uses g-functions computed with pygfunction [19]. The borehole thermal resistance is computed on an hourly basis, varying both the resistance inside the U-tube due to varying thermal properties and flow rates, and in the annulus, where the thermal resistance, driven by buoyancy, depends on both the heat transfer rate and annulus temperature. The thermal resistance inside the U-tube is based on an analytical expression for laminar flow, below Re=2300; above Re=3000 the Gnielinski correlation is used. In between a cubic spline fit is used to give a smooth, continuous function with a continuous derivative (see Figure 2 below). In the annulus, the correlations developed by Spitler, et al. [7] are utilized to determine the convection coefficients and annulus thermal resistance. The borehole thermal resistance is then determined by adding the convective resistance inside the U-tube, the conductive resistance of the U-tube, and the convective resistance in the annulus.

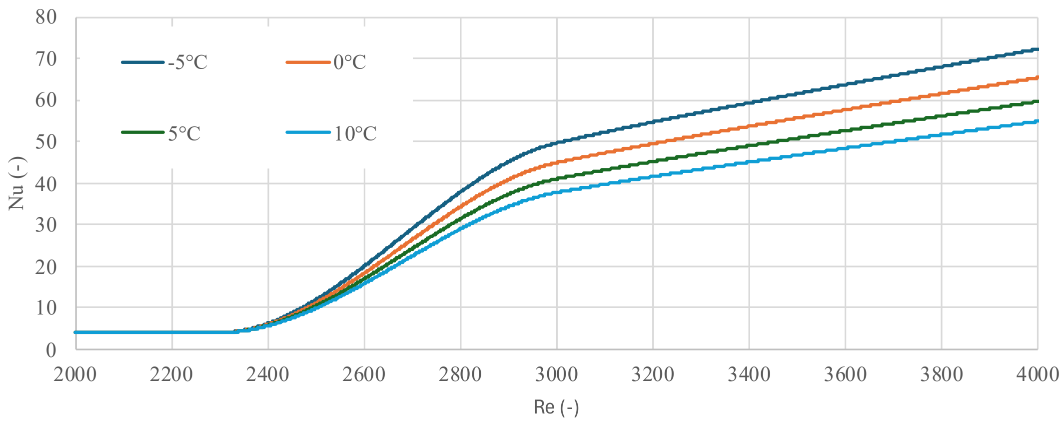

Figure 2. Nusselt Number vs. Reynolds Number for four fluid temperatures

2.4. System Simulation

As will be discussed in section 3, multiple system simulations were utilized, but for the sake of brevity, only the most complex one will be discussed in detail. This would be the simulation that utilizes a detailed heat pump model with auxiliary resistance heating. The system volumetric flowrate is variable to maintain a 3°C temperature difference across the brine-side of the heat pump under an hour's peak conditions.

During each hourly timestep, the system simulation determines the required mean fluid temperature inside the U-tube and volumetric flowrate to match the BHE and heat pump heat extraction and maintain a temperature difference across the BHE of 3°C under peak conditions. The solution for each timestep is found utilizing nested calls to SciPy's fsolve nonlinear root solver [20]. fsolve is also called with three different initial values for the fluid temperature: -10°C, 0°C, and 10°C. The nested calls (rather than one call with two variables) and multiple starts were to increase numerical stability for each timestep at the cost of computation time.

The current BHE heat extraction (Q_{BHE}^{n}) is determined with equation 2:

$$Q_{BHE}^{n} = \frac{T_{f,guess}^{n} - H_{g}^{n}}{C_{g}^{n} + R_{b,n}^{*}} \tag{2}$$

Where $T_{f,guess}^{n}$, is the current guess at the mean fluid temperature in the U-tube at time step n, H_{g}^{n} and C_{g}^{n} are constants related to the g-function at the current time step, and $R_{b,n}^{*}$ is the calculated effective borehole resistance. The g-function constants are only dependent on the g-function and the previous timestep, so will not be discussed in detail. Effective borehole resistance is calculated based on the model discussed in Section 2.3. The groundwater borehole model requires the BHE heat extraction to be known to determine the annulus fluid temperature in the borehole. To increase numerical stability, the borehole effective resistance is calculated with BHE heat extraction from the previous timestep.

The remaining simulation calculations focus on the heat pump model. The complexity of this step comes in the determination of the compressor speed for the heat pump. The extreme cases where the compressor can run at the minimum or maximum speed are quite trivial (and discussed in detail at the end of section 2.2). Determining the compressor speed requires solving Equation 3.

$$\frac{Q_{heating}}{C_{h,0} + C_{h,1}T_{brine}^{n} + C_{h,2}T_{supply,htg.}^{n} + C_{h,3}\omega^{n} + C_{h,4}(\omega^{n})^{2}} + \frac{Q_{dhw}}{C_{h,0} + C_{h,1}T_{brine}^{n} + C_{h,2}T_{supply,dhw}^{n} + C_{h,3}\omega^{n} + C_{h,4}(\omega^{n})^{2}} = 1 \tag{3}$$

This equation has four solutions; however, for the range of reasonable inputs, only one solution provides a positive compressor speed. This solution is provided below in Equations 4-9.

$$C_{1} = C_{h,0} + C_{h,1}T_{brine}^{n} + C_{h,2}T_{supply,htg.}^{n} \tag{4}$$

$$C_{2} = C_{h,0} + C_{h,1}T_{brine}^{n} + C_{h,2}T_{supply,dhw.}^{n} \tag{5}$$

$$B = (C_{1} + C_{2}) - (Q_{heating} + Q_{dhw}) \tag{6}$$

$$C = C_{1}C_{2} - (Q_{dhw}C_{1} + Q_{heating}C_{2}) \tag{7}$$

$$Q_{s} = \frac{-B + \sqrt{B^{2} - 4C}}{2} \tag{8}$$

$$\omega^{n} = \frac{-C_{h,3} + \sqrt{C_{h,3}^{2} + 4C_{h,4}Q_{s}}}{2C_{h,4}} \tag{9}$$

Once the compressor speed is known, the heat pump heat extraction can be determined by subtracting the heating and domestic hot water energy consumptions from their respective heat transfers. Lastly, the maximum temperature difference over the hour is determined by dividing the maximum heat extraction rate (either during the heating or domestic hot water load) by the brine volumetric heat capacity and volumetric flowrate. It should be noted that this is somewhat of a compromise because the model is hourly. The heat pump could adjust multiple times over the hour based on changes in loads. This leads to the actual experienced temperature difference across the BHE in the simulation frequently falling below 3°C due to two effects. This is discussed further in Section 3.3.

2.5. Sizing the borehole heat exchanger

The borehole heat exchanger is sized by adjusting the length so that the minimum mean fluid temperature goes no lower than -1°C over a 10-year hourly simulation. Due to the imbalanced loads used in this study, the sizing/temperature differences could be even more pronounced than shown here; however, computation time constraints prevented broader simulation horizons. An hourly simulation is chosen here instead of a hybrid time-step simulation [21] to see the effects of the modeling variations without having to make further approximations, e.g. creating a method to approximate the heat pump performance over a monthly time step. The sizing was performed by simulating GHEs with 12.5 m increments between 100 m and 200 m. Then the sized length was estimated with interpolation (and rounded to the nearest decimeter). Average ground temperature surrounding the borehole varies with depth, but for the range of depths in this study, the expected variation might be inferred from temperature measurements in the Stockholm area [22] to be about 0.2°C. For this study, the undisturbed ground temperature was considered to be uniform.

3. Results

In Section 3.1, we report verifications of the heat pump model, groundwater-filled borehole model, and the overall system simulation. Then, in order to investigate the effect of considering variable borehole thermal resistance and variable heat pump performance, six cases have been considered, roughly in order of decreasing complexity:

- Case 1. Detailed modeling of the heat pump, including auxiliary electric heating when the load exceeds the vapor compression cycle heating capacity, and groundwater filled borehole, using the standard control of the brine pump to maintain a temperature difference of 3°C.
- Case 2. Same as Case 1, except the brine pump maintains a fixed flow rate of 0.5 L/s. This case was chosen for comparison to Case 1, where the fluid in the U-tube is almost always in laminar flow conditions.
- Case 3. Same as Case 2, but instead of modeling the heat pump, a fixed SCOP of 4.12 given by the manufacturer [23] is used to represent the heat pump. For domestic hot water heating a fixed COP of 2.7 is used. In this case, auxiliary heating is not modeled.
- Case 3b. Same as Case 3, but the maximum vapor compression cycle heating capacity is determined at a heat pump entering temperature of -5°C and supply temperature of 55°C at full compressor speed (which is 5600W). When the heating load exceeds this calculated value, auxiliary heating is used.
- Case 4. Same as Case 3, but instead of modeling variable borehole thermal resistance, a nearly fixed value based on an equivalent water thermal conductivity of 1.25 W/(m·K) is used. (There are very minor variations due to changes in temperature dependent fluid properties of the heat carrier fluid.) This case corresponds to typical Swedish design assumptions.
- Case 4b. Same as Case 4, but, like Case 3b, auxiliary electric resistance heating is modeled.

The above cases are used first to investigate differences in size based on the different approaches. Then, the calculated system performance will be compared by using the approach for each of the six cases with the respective sizes determined with each approach.

3.1. Model and simulation verification

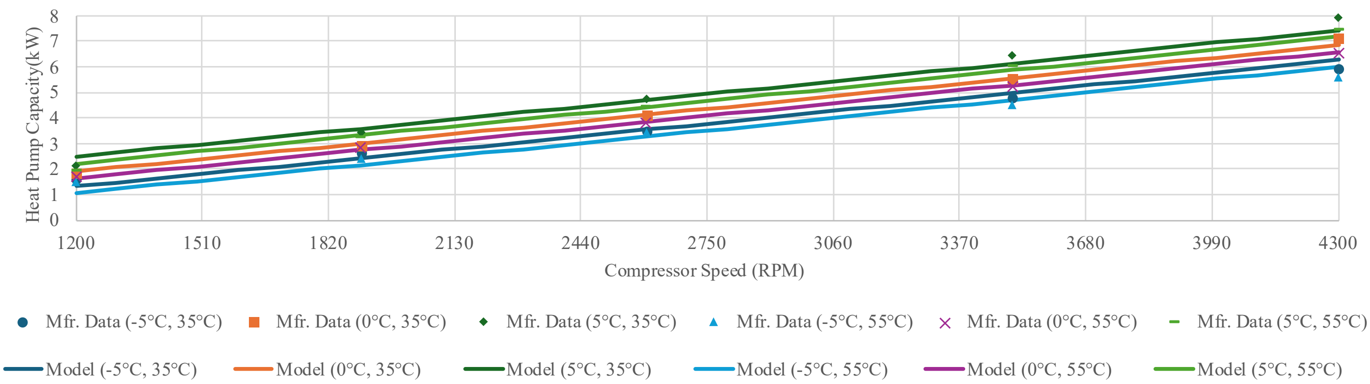

Figure 3 Heat pump capacity model

Figures 3 and 4 illustrate the effectiveness of the capacity and COP fit against the manufacturer-provided data. The capacity fit has an RMSE of 226W across the manufacturer data. The COP fit has an RMSE of

0.15. The manufacturer data contained heat capacity and power consumption for five compressor speeds, three incoming brine temperatures (-5°C, 0°C, and 5°C), and two supply temperatures (35°C and 55°C). The series in Figures 3 and 4 indicate their respective temperatures with paired temperatures (shown in the series names). For example, "(-5°C, 35°C)" would indicate that a series has a brine temperature of -5°C and supply temperature of 35°C.

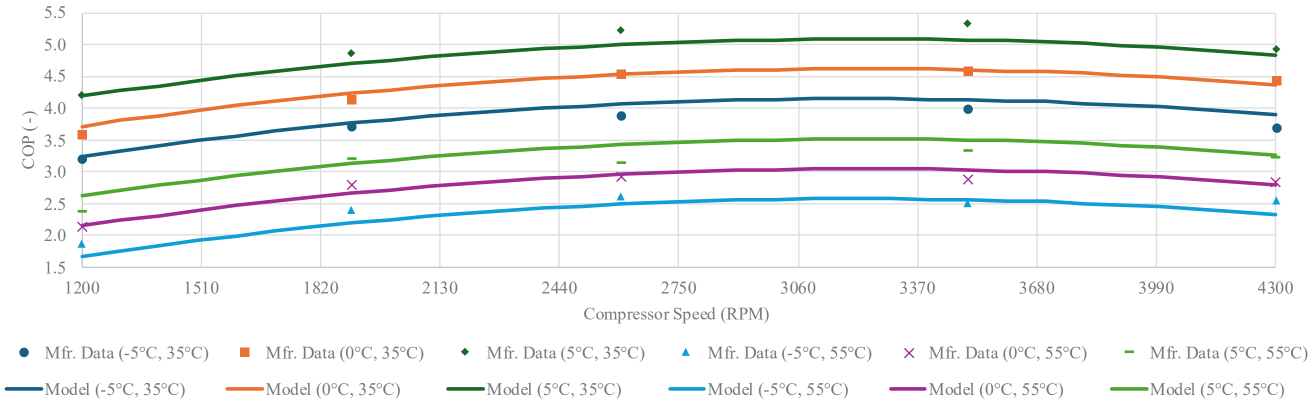

Figure 4 Heat pump COP model

Figure 5 below compares the groundwater filled borehole model from this paper with the TRT results utilized by Spitler et al. [7] to develop their convection correlation for groundwater-filled boreholes. It contains results for Tests 1, 4, and 5. The results match rather closely (especially Tests 1 and 4). The results for Test 5 are still close but seem to suffer from the unsteadiness present during the first 48 hours.

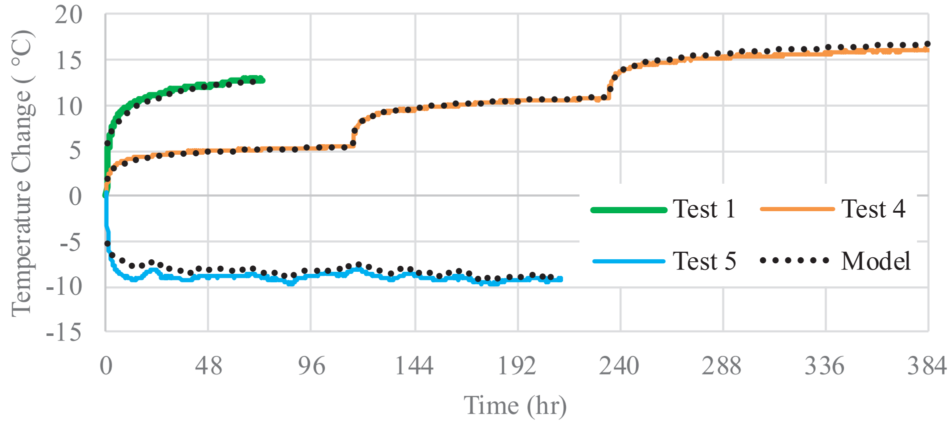

Figure 5. Groundwater-filled borehole test results

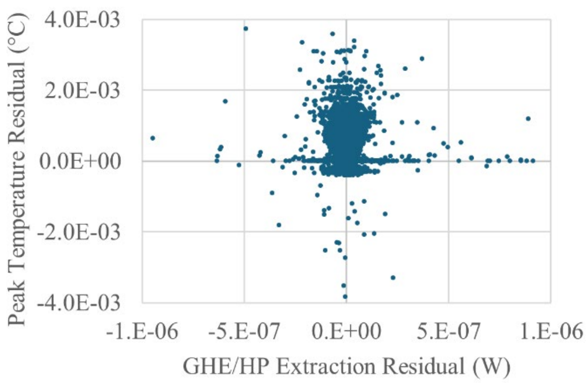

Figure 6. Case 1 simulation solver residuals

Lastly, to demonstrate that the integrated heat pump system model functions as expected, Figure 6 contains the residuals for the Case 1 simulation. All time steps had peak temperature differences within 0.01°C of the 3°C target, and all but three time-steps had differences between BHE and heat pump heat transfer rates within 10^{-6}W of each other. Three hours in 10 years had slightly larger differences, up to 5W. Given the level of heat extraction, on the order of a few kilowatts, these slightly larger residuals are also acceptable.

3.2. Sizing comparison

Figure 7 shows the size results for the six cases. The starkest difference is the difference between Case 1, where the flows are set to maintain a brine temperature difference of 3°C, and Case 2 where the flows are kept constant at 0.5 L/s. This is due to a large difference in effective borehole resistance caused by the flow in Case 1 often being laminar, while in Case 2 it is in the transition region. This will be discussed in detail in the following section. The difference between 2 and 3a is smaller, suggesting that using the two fixed COPs for building heating and domestic hot water heating is a reasonable approximation. Cases 3b and 4b have slightly lower design lengths than cases 3a and 4a, respectively, due to the use of electric resistance heating in cases 3b and 4b. For all cases with electric resistance heating (1, 2, 3b, and 4b) the next section will show that it is used infrequently, so it only has minor effects on sizing and energy consumption. Cases 4a and 4b have higher design lengths than 3a and 3b due to the effective water conductivity predicting higher borehole thermal resistances than the groundwater-filled borehole model.

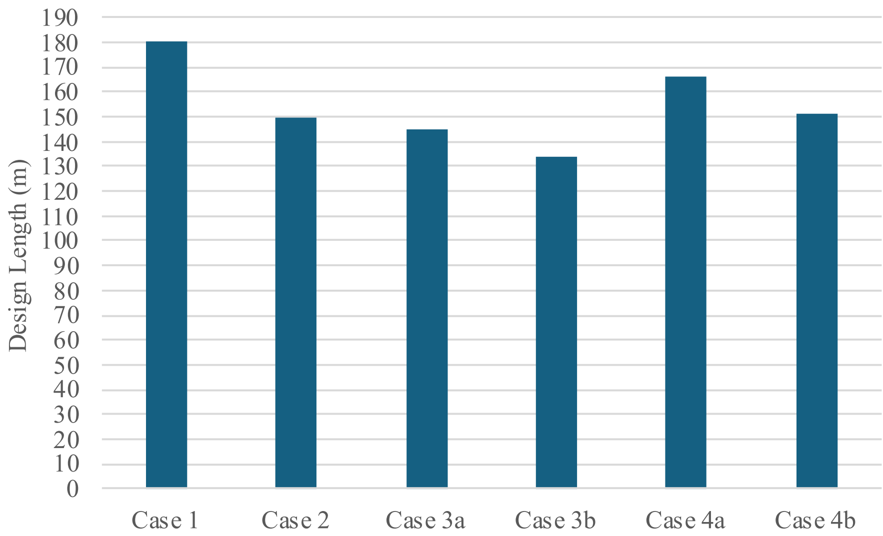

Figure 7. Sized lengths of the six cases

3.3. System performance comparison

In this section, we compare results between the different cases for the 10th year of operation. Figure 8 (Left) illustrates the effective borehole resistance for the six cases. Figure 8 (Right) shows the ratio between the effective borehole resistance and the local borehole resistance. This is a measure of the amount of short-circuiting that occurs. In these plots, Cases 3a and 3b are condensed into a single series, as are 4a and 4b, since they are nearly identical. Case 1 has the highest effective resistances due to mostly laminar flow in the U-tube, which is exacerbated by the high amount of short circuiting that occurs with low flows. Where the flow in Case 1 is high enough to cross into the transition region, the resistance can be seen to spike downward. However, for most of the hours it is much higher. Figure 8 (Left) also demonstrates the highly variable resistance of the groundwater-filled boreholes (Cases 1 -3) compared to Case 4 where the groundwater-filled borehole resistance is approximated as if it were a grouted borehole.

Figure 9 demonstrates the reason behind the increased short-circuiting and borehole resistance in the most complex model (Case 1). Figure 9 (Left) shows the Reynolds numbers for four of the six cases (the four Case 3 and 4 Cases have been combined like Figure 8). Cases 2-4b have nearly identical Reynolds numbers with some small variation due to differences in mean fluid temperatures; however, Case 1 has significantly lower Reynolds numbers. As seen in Figure 9 (Right), this is due to a volumetric flowrate that is consistently below the 0.5 L/s constant flowrate used for the other five cases. The control scheme is trying to maintain a peak temperature difference of 3°C which never requires a flowrate above ~0.4 L/s for this given loading scenario over a 10-year period.

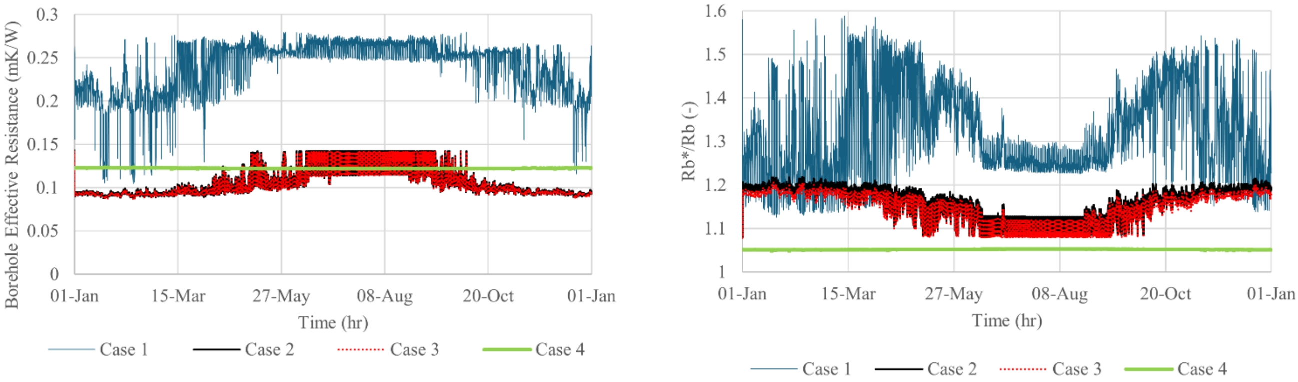

Figure 8. Borehole resistance comparison: Effective resistance (Left) and Ratio of effective to local resistance (Right)

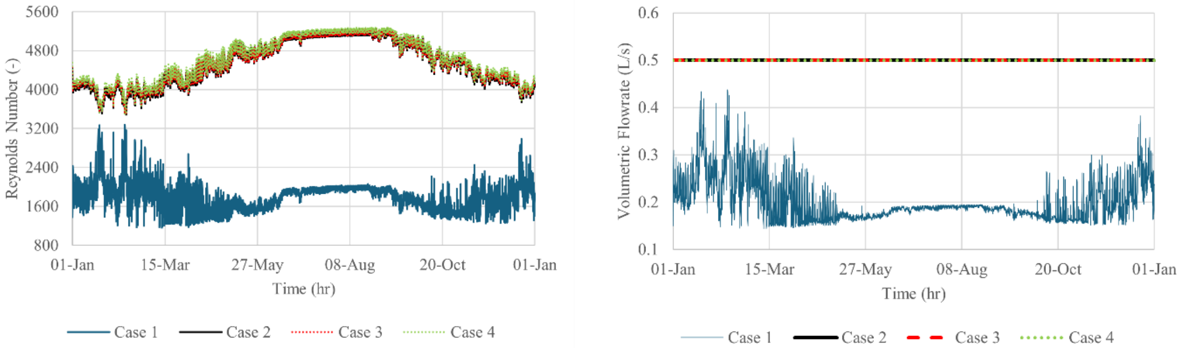

Figure 9. Reynolds Number (Left) and Volumetric flowrate comparison (Right)

These simulation differences also impact the estimated energy consumption across the six cases. Figure 10 compares the total energy consumption for the 10-year simulation broken down by category. To explore the differences, we added an additional case, Case 1*, which is used to examine the effect of using common Swedish assumptions (COP, flow rate, and borehole resistance all constant) to design the BHE. Specifically, Case 1 is modeled with the borehole length sized with Case 4a. Of interest is how using common assumptions may affect performance vs. considering variable flow, COP, and borehole resistance.

To fairly compare the cases, extra energy consumption due to using a higher flow rate in Cases 2-4b was approximated. This is labeled “Pump Energy Offset”, and it is an estimate of the pumping energy not accounted for in the base Case 2-4b models. The additional pumping energy (compared to Case 1) is calculated based on flow rate (varying for Case 1; 0.5 L/s for Cases 2-4b) and assuming that the circulating pump has an efficiency of 20%.

Accounting for variable flow, COP, and borehole resistance for this system shows markedly lower energy consumption than the other cases, whether the BHE is sized with Case 1 or Case 4a. The detailed simulation shows that using the shorter BHE only increases energy consumption by less than 1%. As shown in Figure 11, the mean fluid temperature does, for some hours, drop below the -1°C design limit. This may result in some ice formation on the outside of the U-tube, but the effects are expected to be minimal, given the extra latent energy given off by ice formation and the higher thermal conductivity of the ice. Case 2, where the flow rate has been maintained at a higher level has lower borehole thermal resistance than Case 1, but total energy consumption is about 5% higher, due to the increased pumping energy not being offset by reductions in the heat pump energy consumption. Resistance heating was barely needed in this scenario, so its contribution to the energy differences is miniscule. Gehlin and Spitler [24] investigated sensitivity of a residential GSHP system to a range of flow rates where there was less sensitivity due to decreases in pumping energy being offset by increases in electric resistance heating. In this paper, the heat pump has adequate capacity such that electric resistance heating is rarely needed, which is why Case 2 shows the increase in energy consumption due to higher flow rates. Cases 3 and 4 show higher energy consumption, because the heat pump often operates with a COP above 4.12.

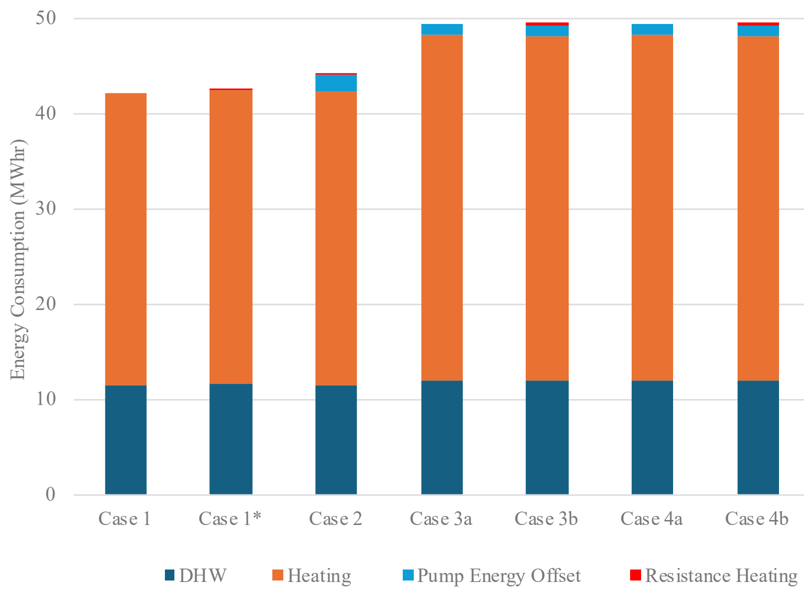

Figure 10. 10-Year Total Energy Consumption Comparison

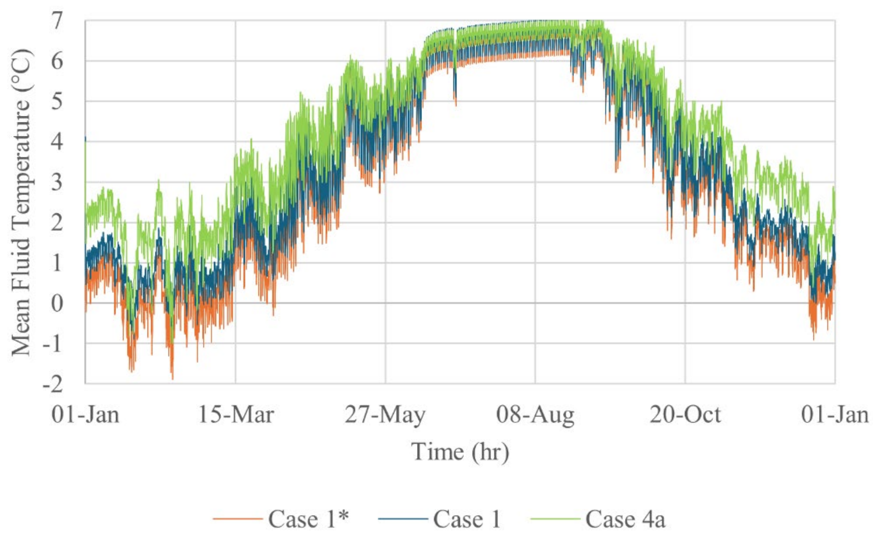

Figure 11. 10th year mean fluid temperatures

Table 1 shows the average monthly electricity consumptions for the 10-year simulation period. To estimate the electricity costs, we used monthly electricity prices (a commonly used rate structure in Sweden) using data from [25] – average annual electricity price for 2024 in Nynäshamn combined with typical monthly variations from the period October 2023-September 2025. The monthly rates are given in the last column of Table 1. The resulting annual energy costs are shown in Figure 13. Despite the monthly variation in electricity cost, the annual electricity costs follow the same trends as the annual energy consumption.

Of particular interest is the question – how much difference would it make if the design length derived from common Swedish design assumptions (Case 4a) were used with the Case 1 approach to determine the energy consumption (Case 1*). Assuming an incremental cost of 350 SEK per meter, Case 1* would save 14.3 m in borehole length, about 5000 SEK in drilling costs. Case 1* would then use about 87 SEK additional electricity per year, so the payback time for drilling to the Case 1 depth instead of the Case 4a depth is about 57 years. Therefore, the Case 4a approach gives an adequate and economic design.

Table 1. Average Monthly Energy Estimates

Month	Energy Consumption (kWhr) Case 1	Case 1*	Case 2	Case 3a	Case 3b	Case 4a	Case 4b	Electricity Cost (SEK/kWhr)
January	626	632	651	756	767	756	750	3.35
February	580	586	604	696	708	696	689	3.00
March	528	533	553	622	622	622	622	2.63
April	375	377	395	426	426	426	426	2.29
May	245	246	259	274	274	274	274	1.78
June	133	133	139	145	145	145	145	1.41
July	89	89	92	93	93	93	93	1.57
August	91	92	95	97	97	97	97	1.56
September	158	159	166	179	179	179	179	1.89
October	350	352	369	402	402	402	402	1.60
November	464	467	487	546	546	546	546	3.58
December	571	575	595	688	688	688	687	3.29
Total	4210	4241	4405	4923	4946	4923	4910	-

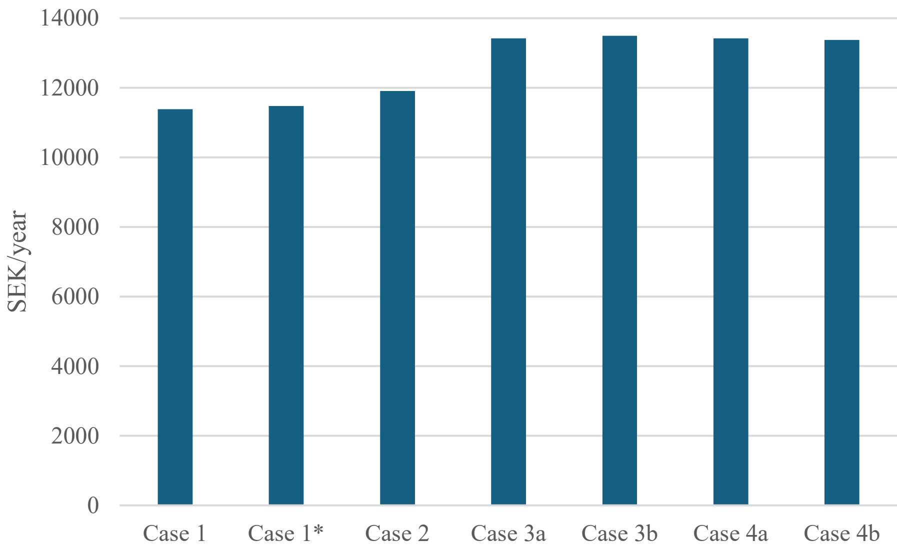

Figure 12. Yearly electrical cost estimate

4. Conclusions and Recommendations

We have examined the effects of a range of design assumptions on the design lengths, energy usage and costs. Case 4a represents common Swedish design assumptions and gives a design length about 8% shorter than what would be achieved from a fully detailed approach, Case 1, with variable heat pump performance, variable borehole thermal resistance, and variable flow that is generally much lower than would be used with Case 4a. The 8% shorter borehole is expected to cause the system to reach mean fluid temperatures slightly below the design limit of -1°C. However, it is anticipated that this will cause no significant problems and that the extra borehole length determined with the Case 1 approach cannot be economically justified.

What are the advantages of the detailed simulation approach? With the work done so far, the detailed approach predicts modestly lower energy consumption, about 14%. This would be advantageous in situations where decisions are being made about system type. E.g., ground-source heat pump vs. air-source heat pump or district heating. These results are generated for a single house/heat pump combination, so further study is warranted. Even better would be detailed field measurements of residential systems that could be used to verify the study results.

Acknowledgements

Heat pump performance data were provided by Thermia.

References

[1] Gehlin, S., O. Andersson, J.-E. Rosberg. 2025. Geothermal Energy Use, Country Update for Sweden. Proceedings EGC2025, Zürich, Switzerland, October 6-10, 2025.
[2] Gustafsson, A.M. and L. Westerlund. 2011. Heat extraction thermal response test in groundwater-filled borehole heat exchanger – Investigation of the borehole thermal resistance. Renewable Energy, 2011. 36(9): p. 2388-2394.
[3] Kjellsson, E. and G. Hellström. 1997. Laboratory study of the heat transfer in a water-filled borehole with a single U-pipe., in Megastock 1997. The 7th international conference on thermal energy storage. 1997: Sapporo, Japan. p. 509-514.
[4] Gustafsson, A.M., L. Westerlund, and G. Hellström. 2010. CFD-modelling of natural convection in a groundwater-filled borehole heat exchanger. Applied Thermal Engineering, 2010. 30(6–7): p. 683-691.
[5] Gustafsson, A. and S. Gehlin. 2008. Influence of Natural Convection in Water-Filled Boreholes for GCHP. ASHRAE Transactions, 2008. 114(1): p. 416-423.
[6] Acuña, J.. 2013. Distributed thermal response tests – New insights on U-pipe and Coaxial heat exchangers in groundwater-filled boreholes. PhD Thesis. 2013, KTH: Stockholm, Sweden.
[7] Spitler, J.D., S. Javed, and R.K. Ramstad. 2016. Natural convection in groundwater-filled boreholes used as ground heat exchangers. Applied Energy, 2016. 164: p. 352-365.
[8] Spitler, J., S. Javed, and R. Grundmann. 2016. Calculation Tool for Effective Borehole Thermal Resistance in Clima 2016. 2016: Aalborg, Denmark.
[9] Todorov, O., et al. 2021. Different Approaches for Evaluation and Modeling of the Effective Thermal Resistance of Groundwater-Filled Boreholes. Energies, 2021. 14(21): p. 6908.
[10] Gehlin, S.E.A. and J.D. Spitler. 2014. Design of Residential Ground Source Heat Pump Systems for Heating Dominated Climates - Trade-Offs Between Ground Heat Exchanger Design and Supplementary Electric Resistance Heating. 2014, ASHRAE: New York.
[11] Gehlin, S.E.A. and J.D. Spitler. 2015. Effects of ground heat exchanger design flow velocities on system performance of ground source heat pump systems in cold climates, in ASHRAE Winter Conference. Chicago, Illinois, January 24-28, 2015.
[12] Javed, S. and J.D. Spitler. 2022. Vertical ground heat exchanger pressure loss – Experimental comparisons and calculation procedures. Geothermics, 2022. 105: p. 102546.
[13] Spitler, J.D., M.Y. Wong, and S.E.A. Gehlin. 2014. Effect of Residential Ground Source Heat Pump System Design on CO_2 Emissions in Sweden, in ASHRAE Annual Conference. 2014: Seattle, Washington, USA.
[14] Claesson, J. and G. Hellström. 2011. Multipole method to calculate borehole thermal resistances in a borehole heat exchanger. HVAC&R Research 17(6): 895-911.
[15] https://www.nrel.gov/buildings/beopt
[16] SVEBY/SMHI. Swedish Climate Files. 2024.
[17] https://thermia.com/products/ground-source-heat-pumps/thermia-calibra/
[18] Björk, E., J. Acuña, E. Granryd, P. Mogensen, J.-E. Nowacki, B. Palm and K. Weber. 2013. Bergvärme på djupet - Boken för dig som vill veta mer om bergvärmepumpar. Stockholm, KTH.
[19] Cimmino, M. 2018. pygfunction: an open-source toolbox for the evaluation of thermal response factors for geothermal borehole fields. eSim 2018, Montreál, IBPSA Canada. 492-501.
[20] Virtanen, P., R. Gommers, T. E. Oliphant, M. Haberland, T. Reddy, et al. 2020. SciPy 1.0: Fundamental Algorithms for Scientific Computing in Python. Nature Methods, 17(3), 261-272.
[21] Cullin, J. R. and J. D. Spitler. 2011. A computationally efficient hybrid time step methodology for simulation of ground heat exchangers. Geothermics 40(2): 144-156.
[22] Gehlin, S. E. A., J. D. Spitler and G. Hellström 2016. Deep Boreholes for Ground Source Heat Pump Systems – Scandinavian Experience and Future Prospects. ASHRAE Winter Conference. Orlando.
[23] https://tcmadmin.thermia.se/docroot/dokumentbank/Calibra_datasheet_13_04_2022_EN.pdf
[24] Gehlin, S. E. A. and J. D. Spitler 2014. Design of Residential Ground Source Heat Pump Systems for Heating Dominated Climates - Trade-Offs Between Ground Heat Exchanger Design and Supplementary Electric Resistance Heating. New York, ASHRAE.
[25] https://nilsholgersson.nu/rapporter/rapport-2025/el-2025/